J|A|C|S
ARTICLES
Published on Web 03/29/2002

Functional Analogue Reaction Systems of the DMSO Reductase Isoenzyme Family: Probable Mechanism of *S*-Oxide Reduction in Oxo Transfer Reactions Mediated by Bis(dithiolene)−Tungsten(IV,VI) Complexes

Kie-Moon Sung and R. H. Holm*

Contribution from the Department of Chemistry and Chemical Biology, Harvard University, Cambridge, Massachusetts 02138

Received December 20, 2001

Abstract: The recent development of structural and functional analogues of the DMSO reductase family of isoenzymes allows mechanistic examination of the minimal oxygen atom transfer paradigm $M^{IV} + QO \rightarrow M^{VI}O + Q$ with the biological metals M = Mo and W. Systematic variation of the electronic environment at the W^{IV} center of desoxo bis(dithiolene) complexes is enabled by introduction of para-substituted phenyl groups in the equatorial (eq) dithiolene ligand and the axial (ax) phenolate ligand. The compounds $[W(CO)_2(S_2C_2(C_6H_4\text{-}p\text{-}X)_2)_2]$ (54−60%) have been prepared by ligand transfer from $[Ni(S_2C_2(C_6H_4\text{-}p\text{-}X)_2)_2]$ to $[W(CO)_3(MeCN)_3]$. A series of 25 complexes $[W^{IV}(OC_6H_4\text{-}p\text{-}X')(S_2C_2(C_6H_4\text{-}p\text{-}X)_2)_2]^{1-}$ ([X,X′], X = Br, F, H, Me, OMe; X′ = CN, Br, H, Me, NH_2; 41−53%) has been obtained by ligand substitution of five dicarbonyl complexes with five phenolate ligands. Linear free energy relationships between $E_{1/2}$ and Hammett constant σ_p for the electron-transfer series $[Ni(S_2C_2(C_6H_4\text{-}p\text{-}X)_2)_2]^{0,1-,2-}$ and $[W(CO)_2(S_2C_2(C_6H_4\text{-}p\text{-}X)_2)_2]^{0,1-,2-}$ demonstrate a substituent influence on electron density distribution at the metal center. The reactions $[W^{IV}(OC_6H_4\text{-}p\text{-}X')(S_2C_2(C_6H_4\text{-}p\text{-}X)_2)_2]^{1-} + (CH_2)_4SO \rightarrow [W^{VI}O(OC_6H_4\text{-}p\text{-}X')(S_2C_2(C_6H_4\text{-}p\text{-}X)_2)_2]^{1-} + (CH_2)_4S$ with constant substrate are second order with large negative activation entropies indicative of an associative transition state. Rate constants at 298 K adhere to the Hammett equations $\log(k^{[X_4,X']}/k^{[X_4,H]}) = \rho_{ax}\sigma_p$ and $\log(k^{[X_4,X']}/k^{[H_4,X']}) = 4\rho_{eq}\sigma_p$. Electron-withdrawing groups (EWG) and electron-donating groups (EDG) have opposite effects on the rate such that $k^{EWG} > k^{EDG}$. The effects of X′ on reactivity are found to be ∼5 times greater than that of X ($\rho_{ax} = 2.1$, $\rho_{eq} = 0.44$) in the Hammett equation. Using these and other findings, a stepwise oxo transfer reaction pathway is proposed in which an early transition state, of primary W^{IV}-O(substrate) bond-making character, is rate-limiting. This is followed by a six-coordinate substrate complex and a second transition state proposed to involve atom and electron transfer leading to the development of the W^{VI}=O group. This work is the most detailed mechanistic investigation of oxo transfer mediated by a biological metal.

Introduction

Our development of structural and reactivity analogues of the active sites of the DMSO reductase (DMSOR) family of molybdoenzymes[1−3] has resulted in the functional oxo transfer reaction systems summarized generally in Figure 1.[4,5] Under the Hille enzyme classification scheme,[1] this family includes DMSO reductase itself and trimethylamine *N*-oxide reductase. Catalytic sites are characterized by *two* pterin dithiolene cofactor ligands bound to the molybdenum atom. In functional systems, we have adopted the minimal reaction paradigm $Mo^{IV} + QO \rightarrow Mo^{VI}O + Q$,[6] and utilized 1,2-dimethylethylene- or (less frequently) 1,2-diphenylethylene-1,2-dithiolate(2−) ligands in complexes whose desoxo and monooxo coordination and metric features are consistent with X-ray absorption and crystallographic results for the enzymes.[7−11] The paradigm now appears to apply to the two most extensively studied DMSO reductases, from *Rhodobacter sphaeroides*[12] and *Rhodobacter capsulatus*.[13] These ligands have been selected in order to provide a credible representation of the structural and electronic features of the native metal coordination. Square pyramidal

* Corresponding author. E-mail: holm@chemistry.harvard.edu.

(1) Hille, R. *Chem. Rev.* **1996**, *96*, 2757−2816.
(2) Romão, M. J.; Knäblein, J.; Huber, R.; Moura, J. J. G. *Prog. Biophys. Mol. Biol.* **1997**, *68*, 121−144.
(3) Kisker, C.; Schindelin, H.; Rees, D. C. *Annu. Rev. Biochem.* **1997**, *66*, 233−267.
(4) Lim, B. S.; Holm, R. H. *J. Am. Chem. Soc.* **2001**, *123*, 1920−1930.
(5) Sung, K.-M.; Holm, R. H. *J. Am. Chem. Soc.* **2001**, *123*, 1931−1943.
(6) Lim, B. S.; Sung, K.-M.; Holm, R. H. *J. Am. Chem. Soc.* **2000**, *122*, 7410−7411.
(7) Czjzek, M.; Dos Santos, J.-P.; Pommier, J.; Méjean, V.; Haser, R. *J. Mol. Biol.* **1999**, *284*, 435−447.
(8) George, G. N.; Hilton, J.; Temple, C.; Prince, R. C.; Rajagopalan, K. V. *J. Am. Chem. Soc.* **1999**, *121*, 1256−1266.
(9) Li, H.-K.; Temple, C.; Rajagopalan, K. V.; Schindelin, H. *J. Am. Chem. Soc.* **2000**, *122*, 7673−7680.
(10) Temple, C. A.; Hilton, J. C.; George, M. G.; Prince, R. C.; Barber, M. J.; Rajagopalan, K. V. *Biochemistry* **2000**, *39*, 4046−4052.
(11) Bray, R. C.; Adams, B.; Smith, A. T.; Bennett, B.; Bailey, S. *Biochemistry* **2000**, *39*, 11258−11269.
(12) Garton, S. D.; Temple, C. A.; Dhawan, I. K.; Barber, M. J.; Rajagopalan, K. V.; Johnson, M. K. *J. Biol. Chem.* **2000**, *275*, 6798−6805.
(13) Bell, A. F.; He, X.; Ridge, J. P.; Hanson, G. R.; McEwan, A. G.; Tonge, P. J. *Biochemistry* **2001**, *40*, 440−448.

10.1021/ja012735p CCC: $22.00

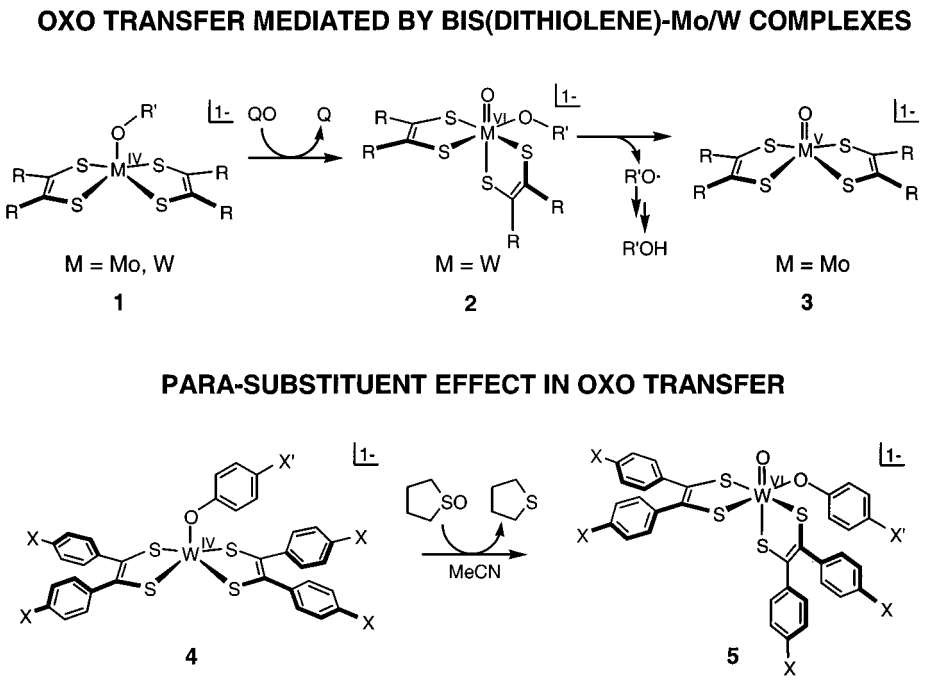

Figure 1. Upper: Depiction of previously studied oxygen atom transfer reactions of *N*-oxides and *S*-oxides mediated by bis(dithiolene)Mo/W complexes **1** and **2** (R = Me, Ph; R′ = Ph, *p*-C_6H_4X', C_6F_5, Pr^i). The $Mo^{VI}O$ reaction product is not stable to an internal redox reaction affording the indicated $Mo^{V}O$ product **3** and an aryloxide radical that abstracts a hydrogen atom, apparently from solvent. Lower: Oxygen atom transfer reactions in this work mediated by $W^{IV,VI}$ complexes **4** and **5** with variable equatorial (X) and axial (X′) para substituents.

desoxo Mo^{IV} complex **1** reacts with *S*-oxides or *N*-oxides to afford distorted octahedral $Mo^{VI}O$ complex **2** and reduced substrate. A typical reaction system contains $[Mo(OPh)(S_2C_2Me_2)_2]^{1-}$, $(CH_2)_4SO$ or Me_3NO, $[MoO(OPh)(S_2C_2Me_2)_2]^{1-}$, and $(CH_2)_4S$ or Me_3N.[4] In this and related systems, the $Mo^{VI}O$ product is not stable and decays to the $Mo^{V}O$ complex **3** by an intramolecular redox reaction forming a $RO^{\bullet}$ radical that abstracts a hydrogen atom, presumably from acetonitrile solvent. The results of a detailed kinetics study of the reduction of *S*-oxide and *N*-oxide substrates have been described.[4]

Given the existence of Mo/W isoenzymes in the DMSOR family,[14−16] a series of bis(dithiolene)W^{IV}, $W^{V}O$, and $W^{VI}O_2$ complexes containing the foregoing ligands has been prepared.[5,17−19] The analogous reaction paradigm $W^{IV} + QO \rightarrow W^{VI}O + Q$ has been followed, with $[W(OPh)(S_2C_2Me_2)_2]^{1-}$, $[WO(OPh)(S_2C_2Me_2)_2]^{1-}$, and substrate comprising a representative reaction system (Figure 1). Tungsten and molybdenum oxo transfer systems with *S*-oxide or *N*-oxide substrates exhibit complementary second-order reactions described by the rate law $-d[M^{IV}]/dt = k[M^{IV}][QO]$ with $k_W/k_{Mo} \approx 2-30$ at 298 K.[4−6,20] The converse rate relationship for substrate oxidation has also been demonstrated.[21] An important difference between the molybdenum and tungsten systems is that monooxo tungsten complex **2** is substantially more stable than is its molybdenum counterpart, thereby simplifying the kinetics analysis.[5]

Oxo transfer reactions mediated by bis(dithiolene)molybdenum and -tungsten complexes exhibit large negative entropies of activation indicative of an associative transition state.[4−6] A transition state of this sort in the reaction system $[Mo(OMe)(S_2C_2Me_2)_2]^{1-}$/$Me_2SO$ follows from density functional calculations and a structure has been presented.[22] In our previous work, we have proposed a stepwise process of oxo transfer consisting of substrate binding through the oxygen atom, S−O bond cleavage, and atom transfer to the metal atom with concomitant oxidation of the latter. Within this manifold of events, the rate-determining event itself remains an open question. To examine this matter, we utilize an extensive series of complexes $[W^{IV}(OR')(S_2C_2R_2)_2]^{1-}$ (**4**) in reactions with $(CH_2)_4SO$ as shown in Figure 1. Here para-substituents X and X′ of the phenyl rings of the equatorial dithiolene and axial phenolate ligands can be varied to provide an extended data set reflecting the dependence of rate constants on electronic factors at the metal center. We have selected the complexes **4** because of manipulatable substitutents, convenient rates, very clean reactions, and the stability of product complexes **5**.

Experimental Section

Preparation of Compounds. All operations were performed anaerobically under a pure dinitrogen atmosphere with use of an inert atmosphere box or standard Schlenk techniques unless otherwise stated. Acetonitrile, dichloromethane, diethyl ether, and THF were purified with an Innovation Technology solvent purification system; 1,4-dioxane and solvents used in column chromatography were of HPLC grade, and deuterated solvents were stored over 4-Å molecular sieves for at least 1 d. Water was purified by a Barnsted NANOpure Diamond system. The compounds $[Ni(S_2C_2Ph_2)_2]$,[23] $[W(CO)_2(S_2C_2Ph_2)_2]$,[17] and $(Et_4N)[W(OPh)(S_2C_2Ph_2)_2]$[5] were prepared as previously described. The compounds 4,4′-dibromobenzil, 4,4′-difluorobenzil, and anisoin (Alfa

(14) Buc, J.; Santini, C.-L.; Giordani, R.; Czjzek, M.; Wu, L.-F.; Giordano, G. *Mol. Microbiol.* **1999**, *32*, 159−168.
(15) Stewart, L. J.; Bailey, S.; Bennett, B.; Charnock, J. M.; Garner, C. D.; McAlpine, A. S. *J. Mol. Biol.* **2000**, *299*, 593−600.
(16) Stewart, L. J.; Bailey, S.; Collison, D.; Morris, G. A.; Garner, C. D. *ChemBioChem* **2001**, *2*, 703−706.
(17) Goddard, C. A.; Holm, R. H. *Inorg. Chem.* **1999**, *38*, 5389−5398.
(18) Sung, K.-M.; Holm, R. H. *Inorg. Chem.* **2000**, *39*, 1275−1281.
(19) Sung, K.-M.; Holm, R. H. *Inorg. Chem.* **2001**, *40*, 4518−4525.
(20) Ueyama, N.; Oku, H.; Nakamura, A. *J. Am. Chem. Soc.* **1992**, *114*, 7310−7311.
(21) Tucci, G. C.; Donahue, J. P.; Holm, R. H. *Inorg. Chem.* **1998**, *37*, 7, 1602−1608.
(22) Webster, C. E.; Hall, M. B. *J. Am. Chem. Soc.* **2001**, *123*, 5820−5821.
(23) Schrauzer, G. N.; Mayweg, V. P. *J. Am. Chem. Soc.* **1965**, *87*, 1483−1489.

Aesar) and 4,4′-dimethylbenzil (Aldrich) were commercial samples and were used without further purification. The compounds $NaOC_6H_4$-*p*-X′ (X′ = CN, Br, H, Me, NH_2) were prepared as described elsewhere.[5] Tetramethylene sulfoxide was distilled over CaH_2 and stored under dinitrogen. Solvent removal and drying steps were performed in vacuo. Because of the large number of related compounds prepared, characterization information (elemental analyses and/or absorption and NMR spectral data) are limited to representative compounds of each type. Further spectral data are available as Supporting Information.[24]

[Ni(S$_2$C$_2$(C$_6$H$_4$-*p*-X)$_2$)$_2$] (X = Br, F, Me, OMe). These complexes were prepared by a procedure analogous to that for [Ni(S$_2$C$_2$Ph$_2$)$_2$][23] with use of 4,4′-disubstituted benzil ((*p*-XC$_6$H$_4$CO)$_2$) or benzoin (*p*-XC$_6$H$_4$CH(OH)COC$_6$H$_4$-*p*-X). A mixture of benzil or benzoin (3−4 g) and 1−1.5 equiv of P_2S_5 in 20 mL of dioxane was heated to reflux at 110 °C for 1−4 h. When the initial yellow suspension became a clear dark brown solution, the latter was cooled to room temperature and filtered to remove an insoluble pale yellow solid. To the filtrate was added a solution of 0.5 equiv of $NiCl_2 \cdot 6H_2O$ per equiv of benzil or benzoin in 1 mL of water, and the mixture was heated to reflux until a black crystalline precipitate developed. The volume of the reaction mixture was reduced to half and the precipitate was collected by filtration, washed with a minimal amount of dioxane, water, methanol, and ether, and dried in air to afford the product as a dark green-brown solid (57−64%).[25] These compounds are satisfactorily identified by spectral data and by electrochemical properties (vide infra).

X = Br. ^{1}H NMR ($CDCl_3$) δ 7.25 (d, 8, J = 8.0 Hz), 7.44 (d, 8, J = 8.0 Hz). Absorption spectrum (dichloromethane) λ_{max} (ϵ_M) 280 (26 600), 323 (34 600), 594 (1530), 864 (21 800) nm.

X = F. ^{1}H NMR ($CDCl_3$) δ 7.01 (t, 8, $J_{H-H} = J_{H-F}$ = 9.2 Hz), 7.35 (dd, 8, J_{H-H} = 8.8 Hz, J_{H-F} = 5.2 Hz). ^{19}F{^{1}H} NMR ($CDCl_3$) δ −111.49. Absorption spectrum (dichloromethane) λ_{max} (ϵ_M) 272 (24 400), 317 (31 000), 594 (1430), 859 (20 600) nm.

X = Me. ^{1}H NMR ($CDCl_3$) δ 2.32 (s, 12), 7.09 (d, 8, J = 8.0 Hz), 7.28 (d, 8, J = 8.0 Hz). Absorption spectrum (dichloromethane) λ_{max} (ϵ_M) 277 (34 200), 321 (38 800), 602 (1862), 877 (28 400) nm.

X = OMe. ^{1}H NMR ($CDCl_3$) δ 3.82 (s, 12), 6.82 (d, 8, J = 8.0 Hz), 7.34 (d, 8, J = 8.0 Hz). Absorption spectrum (dichloromethane) λ_{max} (ϵ_M) 301 (28 000), 335 (20 100), 629 (1230), 928 (20 400) nm.

[W(CO)$_2$(S$_2$C$_2$(C$_6$H$_4$-*p*-X)$_2$)$_2$] (X = Br, F, OMe, Me). These compounds were synthesized by a procedure similar to that for [W(CO)$_2$(S$_2$C$_2$Ph$_2$)$_2$].[17] A mixture of [W(CO)$_3$(MeCN)$_3$] (0.8−1.4 mmol) and [Ni(S$_2$C$_2$(C$_6$H$_4$-*p*-X)$_2$)$_2$] in a 1:4 mol ratio was suspended in 50 mL of dichloromethane. A dark violet or purple solution developed immediately. The reaction mixture was stirred for 24 h, the volume of the reaction mixture was reduced to 2−3 mL in vacuo, and the concentrated solution was eluted on a silica gel column in dichloromethane to remove an insoluble major impurity. A second column chromatography with an ether/pentane eluant system led to the separation of a dark violet or purple band, which was collected. The solvent was removed to give the product as a black or dark violet solid (54−60%). The chromatographic steps were performed in air.

X = Br. Chromatography: ether/*n*-pentane = 1/9 (v/v), R_f = 0.90. IR (KBr) υ_{CO} = 2032 (vs), 1985 (s) cm^{-1}. ^{1}H NMR (acetone-d_6) δ 7.56 (d, 8, J = 8.8 Hz), 7.28 (d, 8, J = 8.8 Hz). Absorption spectrum (THF) λ_{max} (ϵ_M) 311 (sh, 18 900), 540 (20 700), 660 (sh, 2330) nm. Anal. Calcd for $C_{30}H_{16}O_2Br_4S_4W$: C, 34.64; H, 1.55; Br, 30.73; S, 12.33. Found: C, 34.57; H, 1.62 Br, 30.57; S, 12.46.

X = F. Chromatography: ether/*n*-pentane = 1/9 (v/v), R_f = 0.87. IR (KBr) υ_{CO} 2034 (vs), 1989 (s) cm^{-1}. ^{1}H NMR (acetone-d_6) δ 7.13 (t, 8, $J_{H-H} = J_{H-F}$ = 9.2 Hz), 7.36 (dd, 8, J_{H-H} = 8.8 Hz, J_{H-F} = 5.2 Hz). ^{19}F{^{1}H} NMR (acetone-d_6) δ −114.81. Absorption spectrum (THF) λ_{max} (ϵ_M) 313 (sh, 14 700), 538 (13 000), 660 (sh, 1780) nm. Anal. Calcd for $C_{30}H_{16}O_2F_4S_4W$: C, 45.24; H, 2.02; F, 16.10; S, 9.54. Found: C, 46.80; H, 3.15 F, 15.70; S, 9.22.

X = Me. Chromatography: ether/*n*-pentane = 1/9 (v/v), R_f = 0.85. IR (KBr) υ_{CO} 2024 (vs), 1974 (s) cm^{-1}. ^{1}H NMR (acetone-d_6) δ 2.33 (s, 12), 7.14 (d, 8, J = 8.8 Hz), 7.20 (d, 8, J = 8.0 Hz). Absorption spectrum (THF) λ_{max} (ϵ_M) 317 (sh, 13 600), 556 (13 400) nm. Anal. Calcd for $C_{34}H_{28}O_2S_4W$: C, 52.31; H, 3.61; S, 16.43. Found: C, 52.48; H, 3.66; S, 16.51.

X = OMe. Chromatography: ether/*n*-pentane = 1/1 (v/v), R_f = 0.94. IR (KBr) υ_{CO} = 2023 (vs), 1974 (s) cm^{-1}. ^{1}H NMR (acetone-d_6) δ 3.83 (s, 12), 6.89 (d, 8, J = 9.2 Hz), 7.24 (d, 8, J = 8.8 Hz). Absorption spectrum (THF) λ_{max} (ϵ_M) 319 (sh, 21 300), 587 (21 000) nm. Anal. Calcd for $C_{34}H_{28}O_6S_4W$: C, 48.35; H, 3.34; S, 15.18. Found: C, 48.52; H, 3.43; S, 15.29.

(Et$_4$N)[W(OC$_6$H$_4$-*p*-X′)(S$_2$C$_2$(C$_6$H$_4$-*p*-X)$_2$)$_2$] (X = Br, F, H, Me, OMe; X′ = CN, Br, H, Me, NH$_2$). Twenty four compounds have been prepared by a procedure analogous to that for (Et$_4$N)[W(OPh)(S$_2$C$_2$Ph$_2$)$_2$][5] from the combination of five dicarbonyl complexes [W(CO)$_2$(S$_2$C$_2$(C$_6$H$_4$-*p*-X)$_2$)$_2$] and five ligands $NaOC_6H_4$-*p*-X′ on a 0.03−0.05 mmol scale. To a suspension of $NaOC_6H_4$-*p*-X′ and 1 equiv of Et$_4$NCl in 0.5 mL of acetonitrile was added a solution of [W(CO)$_2$(S$_2$C$_2$(C$_6$H$_4$-*p*-X)$_2$)$_2$] in 1.5 mL of THF. The color of the solution changed to brown instantly and the solvents were evaporated. The resulting dark brown solid was redissolved in a minimal volume of acetonitrile, filtered, and recrystallized by addition of ether. Products were obtained as black or dark brown crystals (41−53%).

X = Br, X′ = H. ^{1}H NMR (CD_3CN, anion) δ 6.58 (d, 2, J = 7.2 Hz), 6.91 (t, 1, J = 7.6 Hz), 7.10 (t, 2, J = 8.4 Hz), 7.23 (d, 8, J = 8.8 Hz), 7.38 (d, 8, J = 8.4 Hz). Absorption spectrum (acetonitrile) λ_{max} (ϵ_M) 307 (35 200) nm. Anal. Calcd for $C_{42}H_{41}NOBr_4S_4W$: C, 41.78; H, 3.42; N, 1.16; Br, 26.49; S, 10.62. Found: C, 41.59; H, 3.36; N, 1.22; Br, 26.56; S, 10.52.

X = F, X′ = H. ^{1}H NMR (CD_3CN, anion) δ 6.58 (d, 2, J = 7.2 Hz), 6.91 (t, 1, J = 7.6 Hz), 6.98 (t, 8, $J_{H-H} = J_{H-F}$ = 8.8 Hz), 7.10 (t, 2, J = 8.4 Hz), 7.31 (dd, 8, J_{H-H} = 8.4 Hz, J_{H-F} = 5.6 Hz). ^{19}F-{^{1}H} NMR (CD_3CN) δ −118.27. Absorption spectrum (acetonitrile) λ_{max} (ϵ_M) 306 (34 200) nm. Anal. Calcd for $C_{42}H_{41}NOF_4S_4W$: C, 52.34; H, 4.29; N, 1.45; F, 7.88; S, 13.31. Found: C, 52.38; H, 4.32; N, 1.51; F, 7.96; S, 13.28.

X = Me, X′ = H. ^{1}H NMR (CD_3CN, anion) δ 2.31 (s, 12), 6.57 (d, 2, J = 8.4 Hz), 6.88 (t, 1, J = 7.2 Hz), 7.05 (d, 8, J = 8.4 Hz), 7.09 (t, 2, J = 7.6 Hz), 7.20 (d, 12, J = 8.0 Hz). Absorption spectrum (acetonitrile) λ_{max} (ϵ_M) 306 (38 800) nm. Anal. Calcd for $C_{46}H_{53}NOS_4W$: C, 58.28; H, 5.63; N, 1.48; S, 13.53. Found: C, 58.12; H, 5.72; N, 1.52. S, 13.45.

X = OMe, X′ = H. ^{1}H NMR (CD_3CN, anion) δ 3.76 (s, 12), 6.57 (d, 2, J = 8.8 Hz), 6.79 (d, 8, 8.8 Hz), 6.88 (t, 1, J = 7.6 Hz), 7.08 (t, 2, J = 8.4 Hz), 7.25 (d, 8, J = 8.8 Hz). Absorption spectrum (acetonitrile) λ_{max} (ϵ_M) 310 (43 400), 492 (sh, 1410), 714 (1020) nm. Anal. Calcd for $C_{46}H_{53}NO_5S_4W$: C, 54.59; H, 5.28; N, 1.38; S, 12.67. Found: C, 54.51; H, 5.35; N, 1.32; S, 12.62.

Kinetics Measurements. All reactions were monitored under anaerobic conditions in acetonitrile solutions with a Cary 3 spectrophotometer operating at 250−900 nm. Reduction reactions of tetramethylene sulfoxide to tetramethylene sulfide by the series of W(IV) complexes were run under pseudo-first-order conditions at 25 ± 0.5 °C. Initial W(IV) concentrations were $[W^{IV}]_0$ = 0.50−1.2 mM in systems containing 150−4000 equiv of TMSO. As the reaction proceeds, the color of the solution changes from yellow-brown to violet. The spectral changes accompanying each reaction are similar; a sharp isosbestic point is observed at 340−350 nm and a distinct band of the product W(VI) complex develops at λ_{max} = 517−520 nm, at which wavelength absorbances were taken for the evaluation of rate constants k_{obs} and $k^{[X_4,X']}$.

(24) See the paragraph at the end of this article for Supporting Information available.

(25) These compounds have been reported to be obtained in higher yield with use of different stoichiometry of reactants in 1,2-diethyl-2-imidazolidinone as solvent: Takuma, K.; Irizato, Y.; Katho, K. PCT Int. Appl. 1990; patent no. WO9012019. However, we were unable to reproduce these results and thus followed the method of Schrauzer and Mayweg.[23]

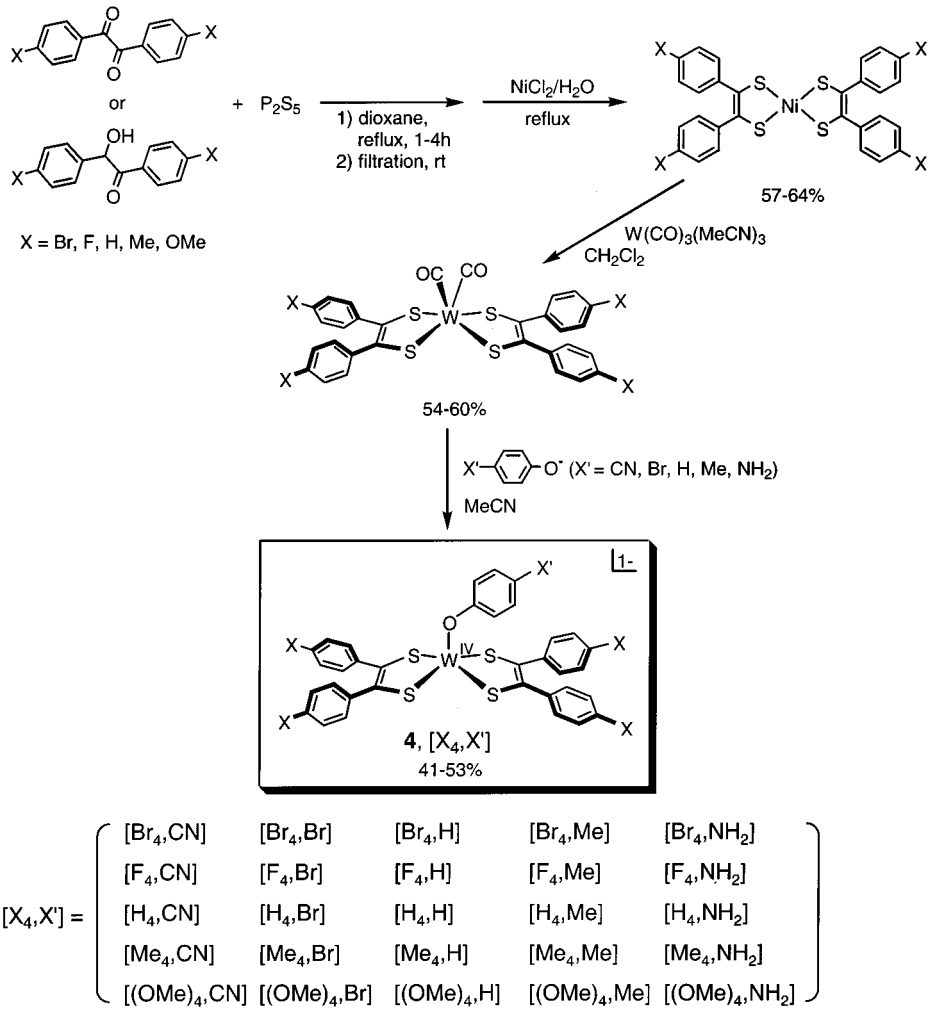

Figure 2. Synthesis of the complexes $[Ni(S_2C_2(C_6H_4\text{-}p\text{-}X)_2)_2]$, $[W(CO)_2(S_2C_2(C_6H_4\text{-}p\text{-}X)_2)_2]$, and $[W(OC_6H_4\text{-}p\text{-}X')(S_2C_2(C_6H_4\text{-}p\text{-}X)_2)_2]$ (**4**). The matrix $[X_4,X']$ of 25 W^{IV} complexes utilized in this work is indicated.

Standard deviations for rate constants were estimated by using a linear least-squares error analysis with uniform weighting of data points.[26] Other details of the experimental procedure and data analysis are described in a previous report.[5]

Other Physical Measurements. Absorption spectra were obtained on Varian Cary 50 Bio or Cary 3 spectrophotometers. ^1H and ^{19}F NMR spectra were taken with a Varian Mercury 400 spectrometer: chemical shifts were referenced to Me_4Si or CCl_3F (^{19}F). IR spectra were measured in KBr pellets with a Nicolet Nexus 470 FT-IR instrument. Electrochemical measurements were performed with a PAR Model 263 potentiostat/galvanostat with a Pt working electrode and 0.1 M Bu_4NPF_6 supporting electrolyte in dichloromethane solutions. Potentials are referenced to the saturated calomel electrode (SCE).

Results and Discussion

Design of Complexes. The oxo transfer reactions mediated by the M = Mo and W complexes in Figure 1 involve species with chelate ring substitutents R = Me or Ph. As has been long recognized with metal dithiolenes, the principal electronic function of R substituents is modulation of redox potentials[27] by influencing electron distribution and frontier orbital energies. For example, potential differences between the R = Me/Ph couples $[Ni(S_2C_2R_2)_2]^{1-/2-}$ (0.32 V) and $[Ni(S_2C_2R_2)_2]^{0/1-}$ (0.28 V)[27] are substantial, as are those for $[WO(S_2C_2R_2)_2]^{1-/2-}$ (0.29 V)[17] and $[W(CO)_2(S_2C_2R_2)_2]^{0/1-/2-}$ (0.21, 0,20 V).[28] In these and all other cases, $E_{Ph} > E_{Me}$ for corresponding couples, consistent with the relative inductive effects of phenyl and methyl groups. In metal dithiolene electron transfer series, the ligands may assume a non-innocent role and, particularly in the more oxidized forms, metal and ligand oxidation states are not well-defined. This is the case in two series, $[Ni(S_2C_2Me_2)]^{2-,1-,0}$ [29] and $[W(CO)_2(S_2C_2Me_2)_2]^{2-,1-,0}$,[28] certain members of which are pertinent to this work. However, in the M = Mo and W complexes **1**−**3**, ring C−C and C−S bond lengths conform to the values expected for double and single bonds, respectively.[5,17−19,30] Consequently, from a structural criterion the ligands behave as classical ene-1,2-dithiolate dianions in the indicated oxo transfer reactions and metal oxidation states of reactant **1** and product **2** are well-defined.

With the foregoing background in mind, we have selected oxo transfer reactions between the desoxo W^{IV} complexes **4** and the constant substrate $(CH_2)_4SO$ in acetonitrile solution for detailed kinetics evaluation. With reference to Figure 2, the complexes $[Ni(S_2C_2(C_6H_4\text{-}p\text{-}X)_2)_2]$ are first prepared by the

(26) Clifford, A. A. *Multivariate Error Analysis*; Halsted Press: New York, 1973.
(27) McCleverty, J. A. *Prog. Inorg. Chem.* **1968**, *10*, 49−221.
(28) Fomitchev, D. V.; Lim, B. S.; Holm, R. H. *Inorg. Chem.* **2001**, *40*, 645−654.
(29) Lim, B. S.; Fomitchev, D. V.; Holm, R. H. *Inorg. Chem.* **2001**, *40*, 4257−4262.

indicated method.[23] Several examples of this general type of complex had been synthesized previously,[23,31,32] and substitutent X varied to tune the energy of the intense near-infrared electronic band characteristic of neutral nickel bis(dithiolene)s. An extensive set has been reported in the Japanese patent literature.[25] The indicated ligand transfer reaction[17] affords $[W(CO)_2(S_2C_2(C_6H_4\text{-}p\text{-}X)_2)_2]$ (54−60%). The carbonyl groups are readily displaced by phenolates to give the desired complexes $[W(OC_6H_4\text{-}p\text{-}X')(S_2C_2(C_6H_4\text{-}p\text{-}X)_2)_2]$ (**4**, 41−53%), which undoubtedly have the square-pyramidal structure of the parent or reference complex $[W(OPh)(S_2C_2Ph_2)_2]^{1-}$.[5] The 25 complexes of interest here are displayed in matrix form in Figure 2. Hereafter, individual complexes are designated as $[X_4,X']$; only the parent $[H_4,H]$ has been prepared previously.

We note the facility with which the synthetic scheme conveniently accommodates independent electronic variation of axial and equatorial ligands within the same molecular framework. Equatorial ligand substitutents are varied four at a time. We are unaware of another confluence of ligand structure and metal that allows a similarly extensive electronic perturbation of a parent molecule under the constraints of effectively constant molecular structure and steric influence on substrate binding.

Linear Free Energy Relationships. Before turning to oxo transfer kinetics, we provide evidence that substituent variation in the groups R = p-C_6H_4X/X' can lead to linear free energy relationships (LFERs). Although redox data abound for one or both steps of electron transfer series 1, there has been only one previous analysis of the dependence of potentials on R groups.[33] Series 2, whose neutral members are precursors to the set $[X_4,X']$, is likewise subject to an analysis of substituent dependence of potentials. The well-defined chemically reversible one-electron redox steps of these series are apparent from the cyclic voltammograms in Figure 3.

$$[Ni(S_2C_2R_2)_2]^0 \leftrightarrow [Ni(S_2C_2R_2)_2]^{1-} \leftrightarrow [Ni(S_2C_2R_2)_2]^{2-} \quad (1)$$

$$[W(CO)_2(S_2C_2R_2)_2]^0 \leftrightarrow [W(CO)_2(S_2C_2R_2)_2]^{1-} \leftrightarrow [W(CO)_2(S_2C_2R_2)_2]^{2-} \quad (2)$$

Values of $E_{1/2}$ for the two series with X = Br, F, H, Me, and OMe are collected in Table 1. The spread in potentials is 190 mV in series 1 and 120−130 mV in series 2. Because potentials are reproducible to ±10 mV, the potential variations are adequate for analysis using Hammett eq 3 and relationships 4 and 5 (T = 298 K). Plots of $(E^X - E^H)/0.059$ vs $4\sigma_p$, shown

$$\log(K_X/K_H) = 4\rho\sigma_p \quad (3)$$

$$\Delta\Delta G^o = -F(E^X - E^H) = -2.303RT\log(K_X/K_H) \quad (4)$$

$$\log(K_X/K_H) = (E^X - E^H)/0.059 \quad (5)$$

in Figure 4, are linear with the slopes ρ_{Ni} = 2.0 and ρ_W = 1.3. Potentials of both steps are taken into account to obtain $E^X - E^H$ values. The substituent effect on the free energy difference

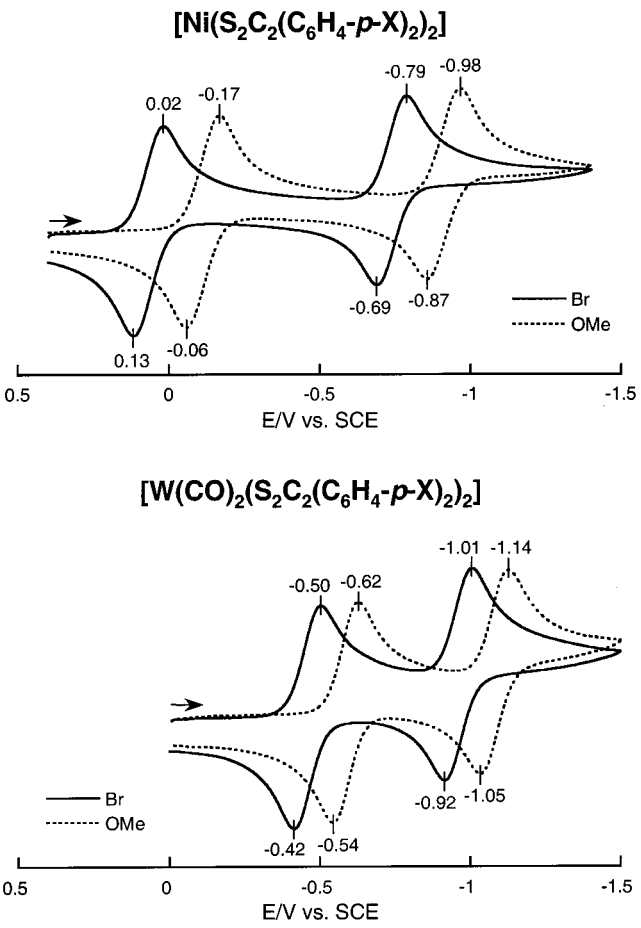

Figure 3. Cyclic voltammograms (100 mV/s) of $[Ni(S_2C_2(C_6H_4\text{-}p\text{-}X)_2)_2]$ (upper) and $[W(CO)_2(S_2C_2(C_6H_4\text{-}p\text{-}X)_2)_2]$ (lower) with X = Br and OMe in dichloromethane, demonstrating the three-member electron-transfer series. Peak potentials are indicated. Complexes with X = F, H, and Me behave similarly.

Table 1. Reversible Redox Potentials for Bis(dithiolene) Nickel and Tungsten Complexes in Dichloromethane

complex	$E_{1/2}$, V[a] (ΔE_p, mV)
Ni	
$[Ni(S_2C_2(C_6H_4\text{-}p\text{-}Br)_2)_2]$	0.075 (110), −0.738(100)
$[Ni(S_2C_2(C_6H_4\text{-}p\text{-}F)_2)_2]$	0.032 (110), −0.794 (110)
$[Ni(S_2C_2Ph_2)_2]$[b]	−0.045 (110), −0.870 (110)
$[Ni(S_2C_2(C_6H_4\text{-}p\text{-}Me)_2)_2]$	−0.097 (140), −0.922 (140)
$[Ni(S_2C_2(C_6H_4\text{-}p\text{-}OMe)_2)_2]$	−0.113 (110), −0.932 (110)
W	
$[W(CO)_2(S_2C_2(C_6H_4\text{-}p\text{-}Br)_2)_2]$	−0.458 (80), −0.971 (90)
$[W(CO)_2(S_2C_2(C_6H_4\text{-}p\text{-}F)_2)_2]$	−0.495 (100), −1.010 (110)
$[W(CO)_2(S_2C_2Ph_2)_2]$[c]	−0.540 (90), −1.060 (90)
$[W(CO)_2(S_2C_2(C_6H_4\text{-}p\text{-}Me)_2)_2]$	−0.568 (90), −1.089 (90)
$[W(CO)_2(S_2C_2(C_6H_4\text{-}p\text{-}OMe)_2)_2]$	−0.578 (80), −1.101 (90)

[a] $E_{1/2} = (E_{pa} + E_{pc})/2$, 100 mV/s, vs SCE, at ~25 °C. [b] In DMF, 0.13 and −0.88 V, respectively, ref 33. [c] In acetonitrile, −0.37 and −0.93 V, repectively, ref 17.

$\Delta\Delta G^o$ is larger in series 1 than series 2 (ρ_{Ni}/ρ_W = 1.5). In the latter, back-bonding of the carbonyl groups may act as a leveling effect in electronic changes produced by variation of X. Values of ν_{CO} are ≳10 cm^{-1} lower for X = Me, OMe than for X = Br, F, consistent with marginally greater back-bonding in molecules with the more electron releasing substituents. The principal point is that electronic effects of substituents are propagated through phenyl groups to the unsaturated chelate

(30) Lim, B. S.; Donahue, J. P.; Holm, R. H. *Inorg. Chem.* **2000**, *39*, 263−273.
(31) Freyer, W. *Z. Chem.* **1980**, *24*, 32−33.
(32) Mueller-Westerhoff, U. T.; Vance, B.; Yoon, D. I. *Tetrahedron* **1991**, *47*, 909−932.
(33) Olson, D. C.; Mayweg, V. P.; Schrauzer, G. N. *J. Am. Chem. Soc.* **1966**, *88*, 4876−4882.

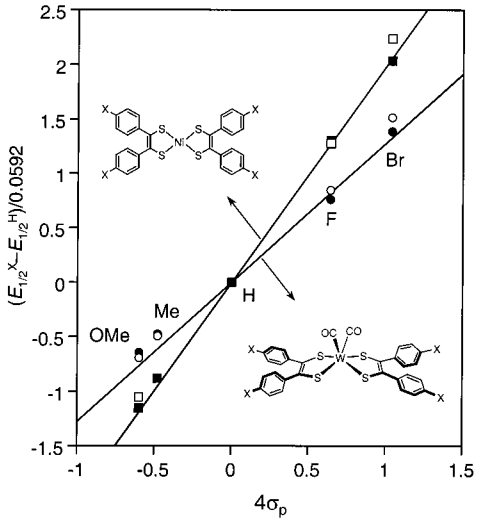

Figure 4. Hammett plots of redox potentials vs $4\sigma_p$ for $[Ni(S_2C_2(C_6H_4\text{-}p\text{-}X)_2)_2]$ and $[W(CO)_2(S_2C_2(C_6H_4\text{-}p\text{-}X)_2)_2]$. The first (■ Ni, ● W) and second (□ Ni, ○ W) potential differences relative to the X = H species are nearly constant and are taken together to generate the linear free energy relationships for the two types of complexes.

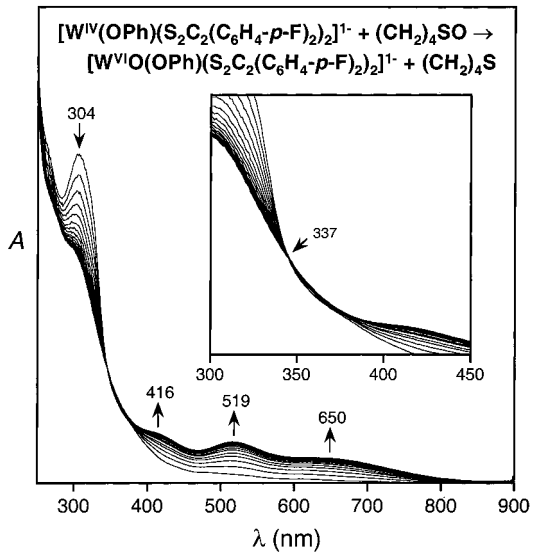

Figure 5. Absorption spectral changes in the pseudo-first-order reaction of $[W^{IV}(OPh)(S_2C_2(C_6H_4\text{-}p\text{-}F)_2)_2]^{1-}$ and $(CH_2)_4SO$ in acetonitrile at 298 K ($[F_4,H]_0 = 0.69$ mM, $[(CH_2)_4SO]_0 = 0.36$ M). Spectra were recorded every 4 min. The inset shows the tight isosbestic point maintained throughout the reaction.

rings of the nickel[29] and tungsten[28] complexes to measurable extents which are manifested as LFERs.

Kinetics and Mechanism of Oxo Transfer. (a) Reaction Systems. Previously, we have shown that the rate constants for reaction 6 (R = Me) in acetonitrile at 298 K adhere to the Hammett equation $\log(k_{X'}/k_H) = \rho\sigma_p$, with the positive slope $\rho = 2.1$ showing that electron-withdrawing groups enhance the rate.[5] Using the same substrate, selected because it offers minimal steric hindrance of any *S*-oxide and reacts ca. 20 times faster than Me_2SO under the same conditions,[5] we provide a more extensive examination of reaction 6 using the complexes

$$[W^{IV}(OC_6H_4\text{-}p\text{-}X')(S_2C_2R_2)_2]^{1-} + (CH_2)_4SO \rightarrow [W^{VI}O(OC_6H_4\text{-}p\text{-}X')(S_2C_2R_2)_2]^{1-} + (CH_2)_4S \quad (6)$$

$[X_4,X']$. The reactions follow the second-order rate law 7 as

$$-d[W^{IV}]/dt = k[W^{IV}][(CH_2)_4SO] \quad (7)$$

previously shown. Kinetics under pseudo-first-order conditions afford linear plots of k_{obs} vs $[(CH_2)_4SO]$, from which the second-order rate constants $k^{[X_4,X']}$ are evaluated. Reactions are notably clean and exhibit tight isosbestic points, as is illustrated by spectrophotometric monitoring of the reaction involving $[F_4,H]$ in Figure 5. Final spectra are closely related to that of $[WO(OPh)(S_2C_2Me_2)_2]^{1-}$ (λ_{max} 408, 514, 637 nm),[5] and provide certain identification of the $[WO(OC_6H_4\text{-}p\text{-}X')(S_2C_2(C_6H_4\text{-}p\text{-}X)_2)_2]^{1-}$ reaction products. While not highly stable, $[WO(OPh)(S_2C_2Me_2)_2]^{1-}$ has been isolated as its Et_4N^+ salt and shown to have distorted octahedral stereochemistry.[5,6] In general, these $W^{VI}O$ complexes are stable over the period of the kinetics measurement, but at longer times (3−5 h after oxo transfer is complete) slowly undergo an autoredox reaction to form blue-green solutions of $[W^{V}O(S_2C_2(C_6H_4\text{-}p\text{-}X)_2)_2]^{1-}$ ($\lambda_{max} \sim 715$ nm). The analogous molybdenum complex $[MoO(OPh)(S_2C_2Me_2)_2]^{1-}$ is too unstable to isolate and also undergoes autoreduction to liberate the phenoxy radical that is detected as phenol.[4] A similar instability pathway is likely for the tungsten complexes. Their decomposition is qualitatively faster with the stronger electron-withdrawing groups X/X′, which presumably effect a more electron-deficient W^{VI} center.

(b) Substituent Dependence of Rate Constants. The rate constant matrix of Table 2 demonstrates that the rates of reaction 6 are sensitive to the substituents X/X′, with relative rate constants reaching a maximum at $k^{[Br_4,CN]}/k^{[(OMe)_4,NH_2]} \approx 390$. Hammett eqs 8 and 9 are used for analysis of the influence of para-substituents on reaction rates. Each column of the rate matrix represents a set of five rate constants that are solely dependent on variable substituent X′ of the axial phenolate ligand at constant X (eq 8). Likewise, each row represents a set of five rate constants that are solely dependent on variable substituent X of the equatorial ligands at constant X′ (eq 9).

$$\log(k^{[X_4,X']}/k^{[X_4,H]}) = \rho_{ax}\sigma_p \quad (8)$$

$$\log(k^{[X_4,X']}/k^{[H_4,X']}) = 4\rho_{eq}\sigma_p \quad (9)$$

The 10 data sets when plotted as eqs 8 and 9 afford the linear relationships evident in Figure 6. Values of ρ_{ax} and ρ_{eq} were obtained from the averaged slopes for axial X′ and equatorial X contributions, respectively. The slopes are positive, indicating that relative to $[H_4,H]$ *an electron-withdrawing group (EWG) accelerates the reaction and an electron-donating group (EDG) has the opposite effect.* The value $\rho_{ax} = 2.1$ matches exactly that for the system $[W(OC_6H_4\text{-}p\text{-}X')(S_2C_2Me_2)_2]^{1-}/(CH_2)_4SO$,[5] supporting the consistency of the results. The much smaller value $\rho_{eq} = 0.44$ with $\rho_{ax}/\rho_{eq} \approx 4.8$ results from the less significant influence of X, which is located farther from the tungsten center than X′. That $k^{EWG} > k^{EDG}$ is further made evident by the three-dimensional plot of rate constants relative to the reference complex $[H_4,H]$ in Figure 7. Complexes lying above the $\log(k^{[X_4,X']}/k^{[H_4,H]}) = 0$ plane carry combinations of X = Br, F and X′ = Br, CN.

(c) Activation Parameters. These parameters were determined for three reactions and are summarized in Table 3 together

Table 2. Second-Order Rate Constants for the Reduction of $(CH_2)_4SO$ Mediated by Bis(dithiolene)W(IV) Complexes $[X_4,X']$ (**4**)[a]

	$k^{[X_4,X']}$ ($M^{-1}s^{-1}$)[b]				
X′	X = Br	X = F	X = H	X = Me	X = OMe
CN	0.51(2)	0.21(2)	0.14(1)	$6.6(1) \times 10^{-2}$	$5.5(1) \times 10^{-2}$
Br	$5.9(1) \times 10^{-2}$	$2.9(1) \times 10^{-2}$	$1.7(2) \times 10^{-2}$	$1.4(1) \times 10^{-2}$	$1.0(2) \times 10^{-2}$
H	$1.4(1) \times 10^{-2}$	$6.6(1) \times 10^{-3}$	$3.0(1) \times 10^{-3}$ [c]	$2.7(3) \times 10^{-3}$	$2.1(1) \times 10^{-3}$
Me	$7.7(1) \times 10^{-3}$	$5.2(1) \times 10^{-3}$	$2.0(5) \times 10^{-3}$	$1.7(4) \times 10^{-3}$	$1.7(1) \times 10^{-3}$
NH_2	$4.7(3) \times 10^{-3}$	$3.2(1) \times 10^{-3}$	$1.8(1) \times 10^{-3}$	$1.4(2) \times 10^{-3}$	$1.3(3) \times 10^{-3}$

[a] In acetonitrile, at 298 K. [b] $-d[W^{IV}]/dt = k^{[X_4,X']}[W^{IV}][(CH_2)_4SO]$ for the reaction series **4** + $(CH_2)_4SO$ → **5** + $(CH_2)S$. [c] Reference 5.

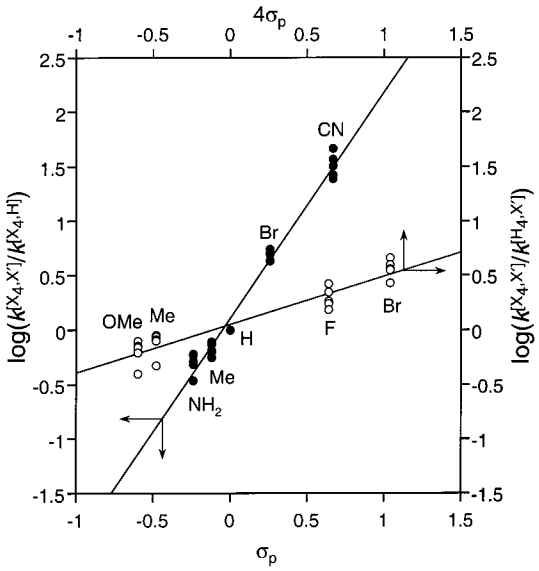

Figure 6. Hammett plots of the relative rates of reaction 6 as $\log(k^{[X_4,X']}/k^{[X_4,H]})$ vs σ_p (●, variable X′ at specified X) and $\log(k^{[X_4,X']}/k^{[H_4,X']})$ vs $4\sigma_p$ (○, variable X at specified X′).

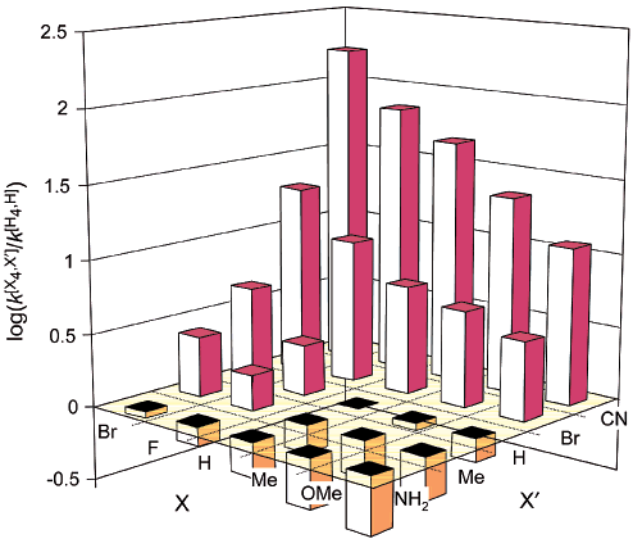

Figure 7. Three-dimensional display of the relative rates of reaction 6 as $\log(k^{[X_4,X']}/k^{[H_4,H]})$ vs X and X′. The black squares lie on the log 1 = 0 plane; symbols extending above and below this plane correspond to complexes $[X_4,X']$ whose rate constants are larger and smaller, respectively, than for $[H_4,H]$.

with those for three reactions of $[W(OC_6H_4\text{-}p\text{-}X')(S_2C_2Me_2)_2]^{1-}$ included for comparison. The slowest and fastest reactions with the constant axial substituent X′ = H were investigated in the $[X_4,H]$ series. As in previous reactions of $[M(OPh)(S_2C_2Me_2)_2]^{1-}$ (M = Mo, W) with *N*-oxides and *S*-oxides,[4-6] activation entropies are large and negative, consistent with an associative

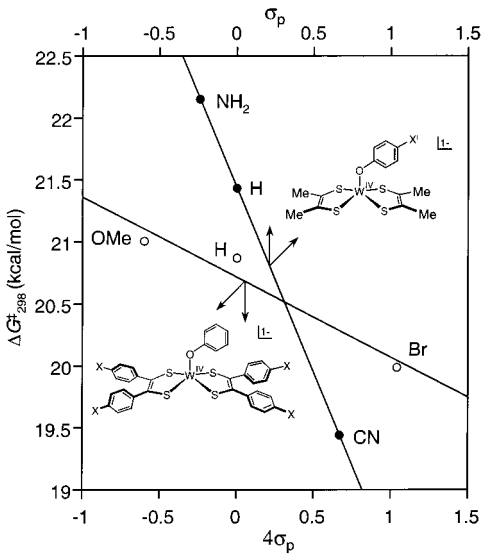

Figure 8. Linear free energy relationships in the reduction of $(CH_2)_4SO$ mediated by $[W(OC_6H_4\text{-}p\text{-}X')(S_2C_2Me_2)_2]^{1-}$ (X′ = CN, H, NH_2) (●) and $[X_4,H]$ (X = Br, H, OMe) (○) in acetonitrile at 298 K.

transition state. Relative rate constants at 298 K are within a factor of 100 for the six reactions, resulting in a variation of only 2.8 kcal/mol in $\Delta G^{\ddagger}_{298}$. However, values of $\Delta H^{\ddagger}$ and $\Delta S^{\ddagger}$ are somewhat differently apportioned in the two sets. For the reactions of $[Br_4,H]$, $[H_4,H]$, and $[(OMe)_4,H]$ values of $|\Delta H^{\ddagger}|$ are lower and those of $|\Delta S^{\ddagger}|$ are higher, such that $T\Delta S^{\ddagger}$ does not vary widely and is 48−57% of $\Delta G^{\ddagger}_{298}$. As anticipated by Hammett plots (Figure 6), there is a linear correlation between $\Delta G^{\ddagger}_{298}$ and substituent parameters of the two sets of complexes in Table 3. These LFERs, demonstrated in Figure 8, emphasize the influence of substituents on rate. Given the linear relationships in Figures 6 and 8, the factors differentiating rates we take to be largely enthalpic in nature. Irregular activation entropies are unlikely to afford linear behavior. We assume the variable enthalpic contributions to apply to all reactions of $[X_4,X']$ complexes.

(d) Mechanistic Considerations. We proceed from the establishment of an associative transition state in and linear free energy relationships for reaction 6. The data of Table 1 clearly reveal that EWGs increase redox potentials. This property of increasing ease of oxidation should extend to desoxo W^{IV}, although it cannot be directly established here because the parent complex $[H_4,H]$ and other $[X_4,X']$ species do not show reversible redox reactions. Rate constants exhibit the order $k^{EWG} > k^{EDG}$, which is opposite to the expected ease of oxidation of W^{IV}, i.e., $E_{EWG} > E_{EDG}$. There being no other suitable measure available, we take this relationship of ground-state potentials to reflect the *intrinsic* relative oxidizability of a W^{IV} center in a transition state, whether by partial charge transfer or discrete

Table 3. Activation Parameters for the Reduction of $(CH_2)_4SO$ Mediated by Bis(dithiolene)W(IV) Complexes

W(IV) complex	k^a ($M^{-1}s^{-1}$)	$\Delta H^{\ddagger}$ (kcal/mol)	$\Delta S^{\ddagger}$ (eu)	$\Delta G^{\ddagger\,a}$ (kcal/mol)
$[W(OC_6H_4\text{-}p\text{-}CN)(S_2C_2Me_2)_2]^{1-\,b}$	$3.5(1) \times 10^{-2}$	10.8(1)	−29(1)	19.4
$[W(OPh)(S_2C_2Me_2)_2]^{1-\,b}$	$9.0(3) \times 10^{-4}$	11.6(4)	−33(1)	21.4
$[W(OC_6H_4\text{-}p\text{-}NH_2)(S_2C_2Me_2)_2]^{1-\,b}$	$3.8(7) \times 10^{-4}$	15(1)	−24(4)	22.2
$[W(OPh)(S_2C_2(C_6H_4\text{-}p\text{-}Br)_2)_2]^{1-}$	$1.4(1) \times 10^{-2}$	8.6(7)	−38(5)	20.0
$[W(OPh)(S_2C_2Ph_2)_2]^{1-}$	$3.0(1) \times 10^{-3\,b}$	9.0(4)	−40(8)	20.8
$[W(OPh)(S_2C_2(C_6H_4\text{-}p\text{-}OMe)_2)_2]^{1-}$	$2.1(1) \times 10^{-3}$	10.9(1)	−34(4)	21.0

[a] In acetonitrile, at 298 K, $-d[W^{IV}]/dt = k[W^{IV}][(CH_2)_4SO]$. [b] Data from ref 5.

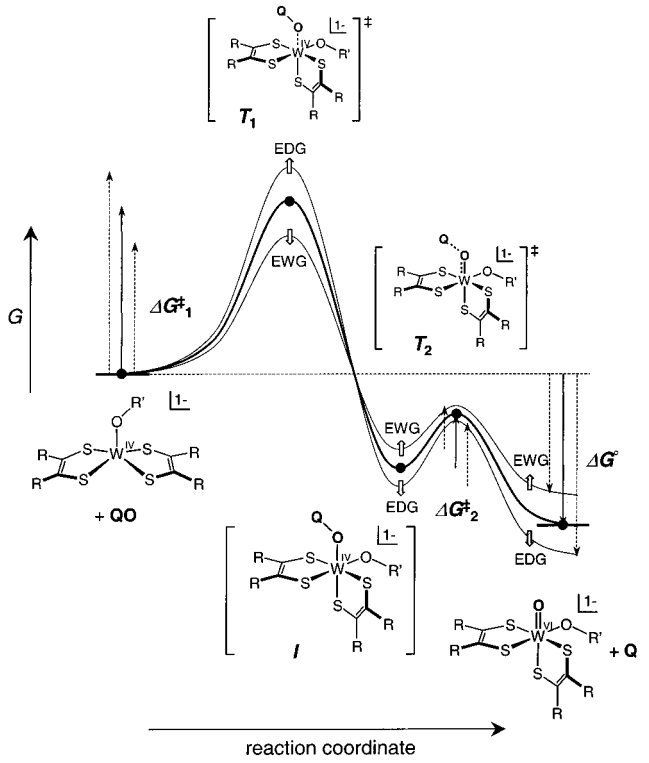

Figure 9. Proposed qualitative reaction coordinate for reaction 6 with schematic representations of transition states ($\boldsymbol{T_1}$, $\boldsymbol{T_2}$) and intermediate (***I***). The thick line refers to a system initially containing reference complex $[W(OPh)(S_2C_2Ph_2)_2]^{1-}$, and other lines to complexes $[W(OR')(S_2C_2R_2)_2]^{1-}$ containing electron-donating groups (EDG) or electron-withdrawing groups (EWD) X/X′ in the substituents R′ = p-C_6H_4X' and R = p-C_6H_4X.

oxidation. The lack of correlation between oxidizability and rate indicates that the event of electron transfer, wherein an oxygen atom is transferred to the metal center with concomitant oxidation to W^{VI} and reduction to oxide, is not, or is not simultaneous with, the rate-determining step. We conclude that the most probable description of the reaction coordinate involves two transition states and one intermediate in the stepwise pathway set out in Figure 9. The first transition state $\boldsymbol{T_1}$ primarily involves $W^{IV}\cdots OQ$ bond-making.[5] The intermediate ***I*** with a discrete W−OQ bond and distorted octahedral stereochemistry is next formed, followed by transition state $\boldsymbol{T_2}$ in which the O−Q bond is largely weakened and the multiply bonded W═O interaction develops. The reaction is completed by separation of reduced substrate Q from the complex, which adopts the stereochemistry of $[WO(OPh)(S_2C_2Me_2)_2]^{1-}$.

The substituent dependence is expressed in the activation free energy to form transition state $\boldsymbol{T_1}$. EWGs would render the W^{IV} center relatively more electrophilic than EDGs, thereby promoting substrate binding and lowering $\Delta G^{\ddagger}_1$ (Figure 9). In the limit of an infinitely strong EWG, ***I*** and $\boldsymbol{T_2}$ are suppressed, and the reaction coordinate reduces to a single transition state. In this interpretation, the rate-determining transition state is early. Its exact geometry cannot be described, but from the Hammond postulate it presumably requires reduction of the chelate ring dihedral angle from the original 128° in [H_4,H]. The extent to which it approaches ca. 100°, as in $[WO(OPh)(S_2C_2Me_2)_2]^{1-}$,[5] is unknown. In support of a transition state with dominant $W^{IV}\cdots OQ$ bond-making in related systems is our previous observation of parallel trends in rate constants for the reaction of $[W(OPh)(S_2C_2Me_2)_2]^{1-}$ and QO and pK_a values of the substrate.[5] Webster and Hall[22] have proposed a transition state model for the simplified reaction $[M(OMe)(S_2C_2Me_2)_2]^{1-} + Me_2SO \rightarrow [MO(OMe)(S_2C_2Me_2)_2]^{1-} + Me_2S$ on the basis of density functional calculations. From theoretical M−$OSMe_2$ and O−S bond lengths, the transition state is substantially biased toward the $\boldsymbol{T_2}$ description. The reaction $[MoO_2(SCH_2CHNH)_2] + Me_3P \rightarrow [MoO(SCH_2CHNH)_2] + Me_3PO$, a model for an actual system,[34] has also been examined by DFT calculations.[35] In both cases a single transition state is considered for the oxo transfer event. Our proposal of two such states follows from the lack of correlation of W^{IV} oxidizability and rate constants.

It is well established that for reduction of the same substrate mediated by strictly analogous bis(dithiolene) molybdenum and tungsten complexes, $k_W > k_{Mo}$, although the effect is not large. Thus for reaction 10 in acetonitrile at 298 K, $k_W/k_{Mo} = 6$ for R = Me and 8.8 for R = Ph.[4−6] For single-turnover reaction 11 of *R. capsulatus* DMSOR isoenzymes, $k_W/k_{Mo} = 17$.[15,16] While

$$[M^{IV}(OPh)(S_2C_2R_2)_2]^{1-} + (CH_2)_4SO \rightarrow [Mo^{VI}O(OPh)(S_2C_2R_2)_2]^{1-} + (CH_2)_4SO \quad (10)$$

$$M^{IV}\text{-DMSOR} + Me_2SO \rightarrow M^{VI}\text{O-DMSOR} + Me_2S \quad (11)$$

we have not carried out a similar study of the molybdenum analogues of reaction 6, a reasonable inference is that the pathway of Figure 9 applies to the reactions of $[Mo^{IV}(OC_6H_4\text{-}p\text{-}X')(S_2C_2R_2)_2]^{1-}$.[4] In this event, the binding of constant substrate to Mo^{IV} is weaker than that for W^{IV}. Structural and mechanistic studies of molybdoenzymes of the DMSOR family have concentrated on catalytic cycles.[12,13,36−39] Little information is available on rate constants for individual steps in the cycle. The intrinsic property $k_W > k_{Mo}$ at parity of substrate and complex structure does not, however, necessarily translate into faster substrate reduction reactions for tungstoenzymes in vivo. Garner and co-workers[16] have provided the instructive demon-

(34) Schultz, B. E.; Holm, R. H. *Inorg. Chem.* **1993**, *32*, 4244−4248.
(35) Thomson, L. M.; Hall, M. B. *J. Am. Chem. Soc.* **2001**, *123*, 3995−4002.
(36) Adams, B.; Smith, A. T.; Bailey, S.; McEwan, A. G.; Bray, R. C. *Biochemistry* **1999**, *38*, 8501−8511.
(37) Canne, C.; Lowe, D. J.; Fetzner, S.; Adams, B.; Smith, A. T.; Kappl, R.; Bray, R. C.; Hüttermann, J. *Biochemistry* **1999**, *38*, 14077−14087.
(38) Pollock, V. V.; Barber, M. J. *Biochemistry* **2001**, *40*, 1430−1440.
(39) Bray, R. C.; Adams, B.; Smith, A. T.; Richards, R. L.; Lowe, D. J.; Bailey, S. *Biochemistry* **2001**, *40*, 9810−9820.

stration that turnover of *R. capsulatus* W-DMSOR is much slower than that of the native Mo-DMSOR. In this case the $M^{VI}O \rightarrow M^{IV}$ step is postulated as rate-determining because of the lower redox potentials of the tungstoenzyme.

Summary. The following are the principal results and conclusions of this investigation.

1. A series of 25 square pyramidal desoxo bis(dithiolene) complexes of the type $[W^{IV}(OC_6H_4\text{-}p\text{-}X')(S_2C_2(C_6H_4\text{-}p\text{-}X)_2)_2]^{1-}$ have been prepared in which equatorial (X = Br, F, H, Me, OMe) and axial (X′ = CN, Br, H, Me NH_2) substituents are independently varied. The complexes provide dissimilarity in electron density at the metal center at essentially constant structure.

2. The complexes $[Ni(S_2C_2(C_6H_4\text{-}p\text{-}X)_2)_2]^{0,1-,2-}$ and $[W(CO)_2(S_2C_2(C_6H_4\text{-}p\text{-}X)_2)_2]^{0,1-,2-}$ constitute reversible electron-transfer series, neutral members of which are synthetic precursors of the complexes in (1). Substituent dependence of redox potentials is demonstrated by a linear free energy relationship between $E_{1/2}$ and the Hammett constant σ_p, with potentials decreasing in the order X = OMe < Me < H < F < Br.

3. Oxo transfer reaction 6 has been examined for the 25 complexes in (1) in acetonitrile. Reactions are first order in W^{IV} and in the constant substrate $(CH_2)_4SO$, and show large negative activation entropies (−34 to −40 eu) consistent with an associative transition state. Rate constants k vary linearly under the Hammett equation $\log(k_X/k_H) = \rho\sigma_p$ with a larger influence of the axial substituent X′ than the more distant equatorial substituent X ($\rho_{ax}/\rho_{eq} = 4.8$). Equivalently, a LFER exists between $\Delta G^{\ddagger}_{298}$ and $\sigma_p(X')$ or $4\sigma_p(X)$. The rate constant order $k^{EWG} > k^{EDG}$ is general and synergistic effects are observed, as indicated by, e.g., $k^{[Br_4,CN]}/k^{[(OMe)_4,CN]} \approx 390$.

4. The results in (2) and (3) lead to the proposal of a stepwise oxo transfer reaction pathway in which the rate-limiting transition state is early and has substantial $W^{IV}-OQ$ bond making character (Figure 9). A six-coordinate intermediate containing bound QO is formed thereafter followed by a second transition state in which most or all of the atom and concomitant electron transfer occurs. From the LFER in (3), $\Delta G^{\ddagger EWG} < \Delta G^{\ddagger EDG}$ and $\Delta G^{\ddagger} \approx \Delta G^{\ddagger}_1 \gg \Delta G^{\ddagger}_2$.

5. Reaction system 6 and others preceding it[4−6] involving structurally and electronically realistic representations of the active sites in the DMSOR enzyme family, inclusive of isoenzymes, are *functional* models of enzyme action.

This work is directed toward a description of the rate-limiting transition state in reaction 6. It is the most detailed investigation yet of the mechanism of oxo transfer mediated by a biological metal. We consider the reaction coordinate in Figure 9 to be intrinsic to the complexes and substrate. The extent to which it might be modified by protein structure and environment remains to be learned. Equally important is the influence of substrate on reaction mechanism. A beginning has been made in our previous investigation, where we note that rate constants do not uniformly correlate with the bond dissociation energy order P−O > As−O > S−O > N−O.[5] This behavior also suggests that the rate-determining step does not involve significant Q−O bond breaking.

Acknowledgment. This research was supported by NSF Grant CHE 98-76457.

Supporting Information Available: Spectroscopic characterization data for 20 complexes of the type $[X_4,X']$ (PDF). This material is available free of charge via the Internet at http://pubs.acs.org.

JA012735P